International Journal of Engineering & Technology, 7 (4.18) (2018) 404-408

International Journal of Engineering & Technology

Website: www.sciencepubco.com/index.php/IJET

Research paper

Electrical Behaviour and Photovoltaic Performance of Poly (ε-caprolactone)-Based Quasi-Solid-State Polymer Electrolyte

N. A. Y. Razamin[1], R. H. Y. Subban[1,2] and Tan Winie[1,2*]

[1] *Faculty of Applied Sciences, Universiti Teknologi MARA, 40450 Shah Alam, Selangor, Malaysia*
[2] *Institute of Science, Universiti Teknologi MARA, 40450 Shah Alam, Selangor, Malaysia*
**Corresponding author E-mail:tanwinie@salam.uitm.edu.my*

Abstract

Quasi-solid-state polymer electrolytes based on poly(ε-caprolactone) (PCL) and dimethylformamide (DMF) with various concentrations of potassium iodide (KI) were prepared and characterized for their electrical properties and the performance in dye-sensitized solar cells (DSSCs). Incorporation of KI increased the conductivity by 3 order of magnitude from 10^{-6} to 10^{-3} Scm^{-1}. The highest conductivity was achieved at 0.2 M of KI. The number, *n* and mobility, μ of ions were calculated by impedance spectroscopy to evaluate the conductivity variation quantitatively. Conduction mechanism of the electrolyte was determined using Jonscher's universal power law. The conduction mechanism was discussed by comparing the behaviour of temperature dependence of exponent *s* with existing theoretical models. The small polaron hopping (SPH) model was found to be the model for conduction mechanism of PCL-DMF-KI electrolyte. DSSC with 0.2 M of KI shows the highest photovoltaic performance, η of 2.72% with short-circuit current density, J_{sc} of 5.56 mA cm^{-2}, open circuit voltage, V_{oc} of 0.72 V and fill factor, *ff* of 69%.

Keywords: *DMF; DSSC; KI; PCL; Polymer Electrolyte*.

1. Introduction

Quasi-solid-state (QSS) electrolyte, also known as semi-solid electrolyte, shares the uniqueness of solid and liquid electrolytes. It consists of a polymeric host, a plasticizing solvent and a conducting salt. The liquid phase of QSS electrolyte provides channels for ionic conduction whereas the polymeric phase holds the liquid in a solid rubbery state and hence prevents the liquid from leaking. QSS electrolyte is usually prepared by incorporating a gelling agent into a liquid plasticizing solvent containing desired salt. Polymer or inorganic fillers can serve as a gelling agent [1-6]. We focus on polymeric gelling agent.

Synthetic polymers such as poly(ethylene oxide) (PEO) [7], poly(vinylidenefluoride-*co*-hexafluoropropylene) (PVdF-HFP) [8], poly(methyl methacrylate) (PMMA) [9] and biopolymers such as chitosan [10], carboxymethyl cellulose (CMC) [11], cyanoethylated hydroxypropyl cellulose (CN-HPC) [12] have been used to prepare QSS electrolytes. In this study, we developed poly(ε-caprolactone) (PCL)-based QSS electrolyte. PCL, the synthetic thermoplastic polymer is non-toxic and biodegradable [13]. It is being used in biomedical applications [14, 15]. PCL contains electron pairs at the ester oxygen that can coordinate with cation of salt. This makes it a candidate as host in QSS electrolyte.

In the preparation of PCL-based QSS electrolytes, dimethylformamide (DMF) and potassium iodide (KI) were employed as the plasticizing solvent and conducting salt, respectively. The optimized electrolyte samples were used in the application of dye-sensitized solar cells (DSSCs). This paper reports the electrical properties of PCL-DMF-KI electrolytes together with the photovoltaic performance of the DSSCs.

2. Experimental

PCL with molecular weight of 80,000 g mol^{-1} (Sigma-Aldrich), DMF and KI with purity > 99% (Systerm) were used as received. Different amounts of KI ranging from 0.0 to 0.5 M were added to the DMF containing fixed amount of PCL, stirred at 50 ^{o}C until "gel-like" electrolyte is formed. Electrical studies were carried out using a HIOKI 3532-50 LCR Hi-tester impedance spectrometer in the frequency range from 50 Hz to 1 MHz.

Titanium dioxide (TiO_2) photoanodes were prepared by coating fluorine-tin oxide (FTO) conducting glass with two layers of TiO_2 and soaking in 3mM N3 dye (cis-bis(isothiocyanato) bis(2,2'-bipyridyl-4,4'-dicarboxylato) ruthenium (II)). Details of preparing TiO_2 photoanode can be obtained from [16]. Platinum (Pt) counter electrodes were prepared by spin-coating a Pt solution on FTO glass and sintered at 450 ^{o}C for 30 min.

Small amount of "gel-like" electrolyte was placed in between TiO_2 photoanode and Pt counter electrode for DSSC assembly. The current-voltage (*J-V*) characteristics of the DSSCs were measured under illumination of 100 mWm^{-2} Xenon light source (Oriel LCS 100) with a Metrohm Autolab potentiostat (PGSTAT128N).

3. Results and discussion

3.1. Conductivity

Fig. 1 shows the temperature dependence of conductivity for PCL-DMF-KI electrolyte. Conductivities of all electrolyte samples are found to increase with temperature. The order of the conductivity

Copyright © 2018 Authors. This is an open access article distributed under the Creative Commons Attribution License, which permits unrestricted use, distribution, and reproduction in any medium, provided the original work is properly cited.

is 0.0 M KI < 0.5 M KI < 0.1 M KI < 0.4 M KI < 0.3 M KI < 0.2 M KI. Presence of KI increases the conductivity. This is because KI provides ions for conduction. The maximum conductivity is achieved at 0.2 M of KI.

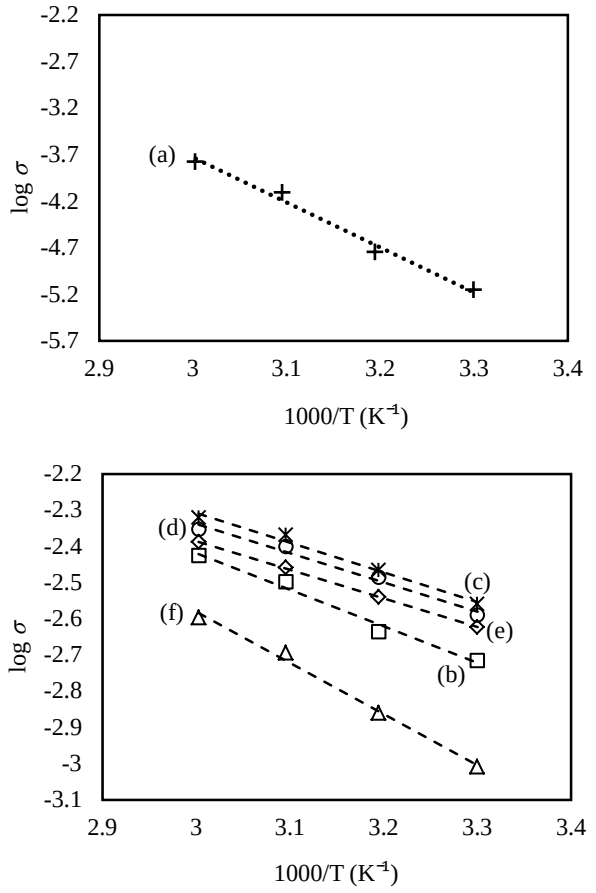

Fig. 1: Temperature dependence of conductivity for PCL-DMF electrolyte containing (a) 0.0 M KI, (b) 0.1 M KI, (c) 0.2 M KI, (d) 0.3 M KI, (e) 0.4 M KI and (f) 0.5 M KI.

Conductivity of an electrolyte depends upon two parameters i.e. number, n and mobility, μ of ions. Determination of n and μ allows a quantitative analysis of the conductivity trend. In this study, the n and μ were determined using impedance spectroscopy.

Fig. 2 shows the Nyquist plots for electrolytes with and without KI. For electrolyte without KI, the Nyquist plot shows a depressed semicircle and a small titled spike (cf. Fig. 2(a)). Thus, the equivalent circuit representation is parallel combination of resistance, R and constant phase element (CPE) with another CPE in series [17]. The real, Z_r and imaginary, Z_i parts of impedance associated to the equivalent circuit are [18]:

$$Z_r = \frac{\frac{1}{R} + Q_1\omega^{\beta_1}\cos\left(\frac{\beta_1\pi}{2}\right)}{\left[\frac{1}{R} + Q_1\omega^{\beta_1}\cos\left(\frac{\beta_1\pi}{2}\right)\right]^2 + \left[Q_1\omega^{\beta_1}\sin\left(\frac{\beta_1\pi}{2}\right)\right]^2} + \frac{1}{Q_2\omega^{\beta_2}}\cos\left(\frac{\beta_2\pi}{2}\right) \quad (1)$$

$$Z_i = \frac{Q_1\omega^{\beta_1}\sin\left(\frac{\beta_1\pi}{2}\right)}{\left[\frac{1}{R} + Q_1\omega^{\beta_1}\cos\left(\frac{\beta_1\pi}{2}\right)\right]^2 + \left[Q_1\omega^{\beta_1}\sin\left(\frac{\beta_1\pi}{2}\right)\right]^2} + \frac{1}{Q_2\omega^{\beta_2}}\sin\left(\frac{\beta_2\pi}{2}\right) \quad (2)$$

where R and Q_1 are the bulk resistance and bulk capacitance of the electrolyte, respectively. Q_2 is the double-layer capacitance at the electrolyte-electrode interface. β_1 is the deviation of the semicircle diameter from the Z_i axis and β_2 is the deviation of the spike from the Z_r axis. ω is the angular frequency.

The Nyquist plots for all KI-containing electrolytes show only tilted spikes (cf. Fig. 2(b)). The equivalent circuit can be represented by a resistor connected in series with a CPE [17]. The Z_r and Z_i can then be expressed as [19, 20]:

$$Z_r = R + \frac{\cos\left(\frac{\beta_2\pi}{2}\right)}{Q_2\omega^{\beta_2}} \quad (3)$$

$$Z_i = \frac{\sin\left(\frac{\beta_2\pi}{2}\right)}{Q_2\omega^{\beta_2}} \quad (4)$$

Equations (1) and (2) were used to fit the Nyquist plot of Fig. 2 (a) while equations (3) and (4) were used to fit the Nyquist plots of Fig. 2 (b). The values of R, Q_1, Q_2, β_1 and β_2 can be obtained by trial and error until the plots are fitted (cf. Table 1).

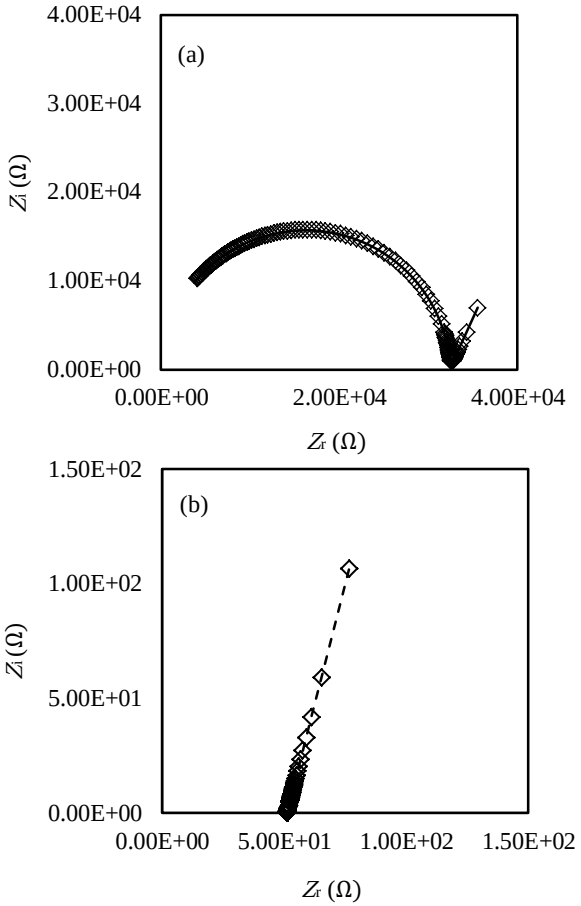

Fig. 2: Nyquist plots of (a) PCL-DMF and (b) PCL-DMF-0.2 M KI electrolytes. 0.2 M KI was selected as representative example for KI-containing electrolytes. Dotted line is plot fitting after equations (1) to (4).

Table 1: The circuit parameters of R, Q_1, Q_2, β_1 and β_2 at room temperature.

KI content (M)	R (Ω)	Q_1 (F)	Q_2 (F)	β_1 (rad)	β_2 (rad)
0.0	32400.0	4.20×10^{-11}	1.96×10^{-6}	0.98	0.73
0.1	75.9	-	9.20×10^{-6}	-	0.82
0.2	36.0	-	3.71×10^{-5}	-	0.81
0.3	52.2	-	4.26×10^{-5}	-	0.81
0.4	52.5	-	2.17×10^{-5}	-	0.83
0.5	121.5	-	5.68×10^{-6}	-	0.85

The obtained value of Q_2 was then used to calculate the ion diffusion coefficient, D according to equation (5) [21].

$$D = \frac{1}{\tau}\left(\frac{\varepsilon_r \varepsilon_0 A}{Q_2}\right)^2 \quad (5)$$

The value of τ can be taken at the frequency at $Z_i \rightarrow 0$ [18]. The dielectric constant of the electrolyte, ε_r can be extracted from the plot of ε_r vs. log f (cf. Fig. 3). A is the electrolyte-electrode contact area and ε_o is the permittivity of free space.

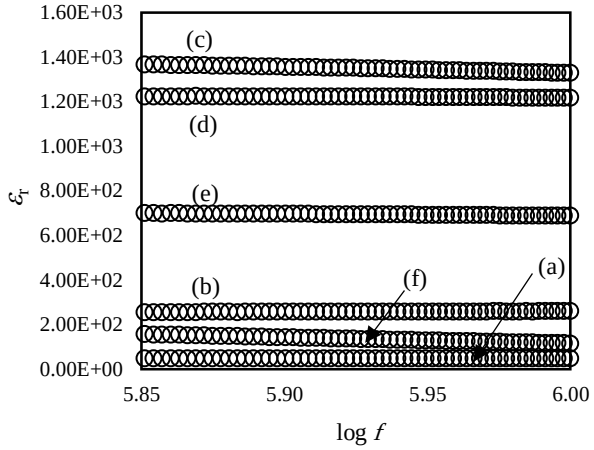

Fig. 3: Frequency dependence of dielectric constant, ε_r for PCL-DMF electrolyte containing (a) 0.0 M KI, (b) 0.1 M KI, (c) 0.2 M KI, (d) 0.3 M KI, (e) 0.4 M KI and (f) 0.5 M KI.

With the known value of D, the n and μ can be calculated according to equations (6) and (7), respectively [21].

$$n = \frac{\sigma k_B T}{e^2 D} \quad (6)$$

$$\mu = \frac{eD}{k_B T} \quad (7)$$

where σ is the conductivity, k_B is the Boltzmann constant and T is temperature in Kelvin. Table 2 lists the calculated values of D, n and μ for PCL-DMF-KI electrolyte at room temperature.

Table 2: The values of room temperature conductivity, σ_{RT}, ε_r, τ, D, n and μ for PCL-DMF electrolytes containing various concentrations of KI.

KI content (M)	σ_{RT} (Scm^{-1})	ε_r (at 700 Hz)	τ (s^{-1})
0.0	4.28 x 10^{-6}	44	8.16x10^{-5}
0.1	1.83 x 10^{-3}	252	1.59x10^{-6}
0.2	2.72 x 10^{-3}	1362	7.76x10^{-7}
0.3	2.66 x 10^{-3}	1219	1.68x10^{-6}
0.4	2.64 x 10^{-3}	695	1.87x10^{-6}
0.5	8.91 x 10^{-4}	152	2.12x10^{-6}

The initial increase of conductivity with incorporation of KI is due to the dissociation of KI to provide K^+ cation and I^- anion for conduction. With increase in the amount of KI, more K^+ and I^- ions are available for conduction (i.e marked by the greater number of n in Table 3). However, beyond 0.2 M of KI, dissociated $K^+$and I^- ions re-associate. This is because as the number of dissociated ions increases, the distance between ions decreases. Consequently, dissociated ions re-associate due to strong coulombic attraction between them. Ion association not only decrease the number of free ions, n but also increase the medium viscosity. An increase in viscosity results in lower mobility of ions, μ. As a result, conductivity decreases beyond 0.2 M of KI.

Table 3 (continue): The values of room temperature conductivity, σ_{RT}, ε_r, τ, D, n and μ for PCL-DMF electrolytes containing various concentrations of KI.

KI content (M)	D (cm^{2}s^{-1})	n (cm^3)	μ (cm^{2}V^{-1}s^{-1})
0.0	3.69x10^{-7}	1.86x10^{18}	1.44x10^{-5}
0.1	2.82x10^{-5}	1.04x10^{19}	1.07x10^{-3}
0.2	2.99x10^{-5}	1.46x10^{19}	1.16x10^{-3}
0.3	2.96x10^{-5}	1.44x10^{19}	1.15x10^{-3}
0.4	2.97x10^{-5}	1.43x10^{19}	1.15x10^{-3}
0.5	2.02x10^{-5}	7.10x10^{18}	7.85x10^{-4}

3.2. Conduction mechanism

The Jonscher's universal law is given as [22]:

$$\sigma(\omega) = \sigma_{dc} + B\omega^s \quad (8)$$

where $\sigma(\omega)$ is the total conductivity, σ_{dc} is the dc conductivity. The ac conductivity is represented by $B\omega^s$ with B being the parameter dependent on temperature and s is the power law exponent with value in the range of $0 < s < 1$. The exponent s can be determined using [23]:

$$\ln \varepsilon_i = ln\frac{B}{\varepsilon_o} + (s-1)\ln \omega \quad (9)$$

where ε_i is the dielectric loss, symbols ε_o and ω have their usual meanings. Fig. 4 presents the plots of ln ε_i vs. ln ω.

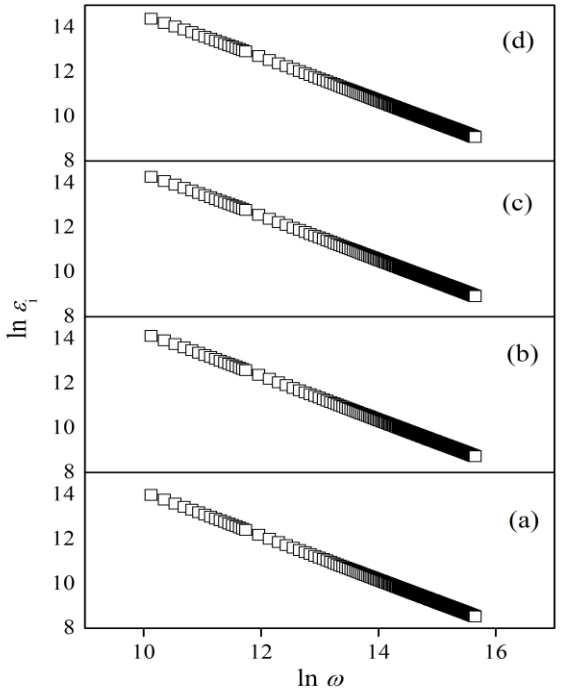

Fig. 4: Plots of ln ε_i vs. ln ω for PCL-DMF electrolyte containing 0.2 M KI at (a) 303 K, (b) 313 K, (c) 323 K and (d) 333 K.

Various theoretical models have been developed to correlate the exponent s with conduction mechanism of an electrolyte. According to the quantum mechanical tunneling (QMT) model, the exponent s is almost equal to 0.8 and increases slightly with temperature or temperature independent [24, 25]. The small polaron hopping (SPH) model predicts the exponent s to be increased with increasing temperature [20, 24]. In the overlapping large polaron tunnelling (OLPT) model, the exponent s decreases with temperature, reaches a minimum and then begin to increase again with temperature [25]. Correlated barrier hopping (CBH) model, on the other hand, predicts the exponent s to be increased towards unity as T→0 K [26].

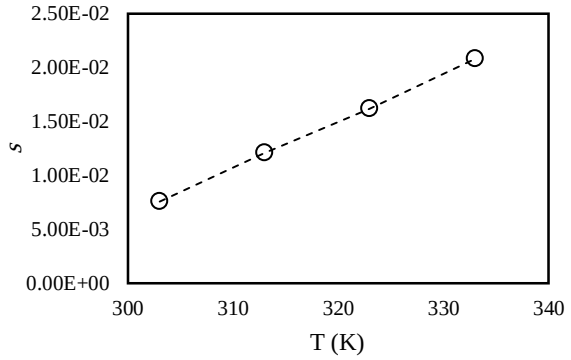

Fig. 5: Variation of the exponent *s* with temperature for PCL-DMF electrolyte containing 0.2 M of KI.

Slope of the plots of ln ε_i vs. ln ω give the values of exponent *s*. From Fig. 5, the exponent *s* is found to increase linearly with temperature. Thus, the conduction mechanism for PCL-DMF-KI electrolyte can be interpreted based on the SPH model. In the SPH model, small polaron is formed upon incorporation of an ion to a site. This results in local lattice distortion. Small polarons are assumed to be localized so that ion hopping is independent on the intersite separation [23].

3.3. Photovoltaic performance

PCL-DMF electrolytes with different KI concentrations were assembled into DSSCs. Fig. 6 presents the J-V characteristics for the DSSCs. The open circuit voltage, Voc and the short-circuit current density, Jsc were obtained from the intercept of the plot on the voltage axis and current density axis, respectively.

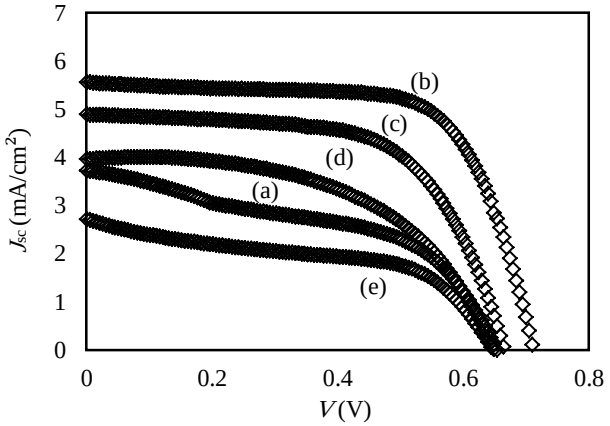

Fig. 6: *J-V* characteristics of DSSCs for PCL-DMF electrolyte containing (a) 0.1 M KI, (b) 0.2 M KI, (c) 0.3 M KI, (d) 0.4 M KI and (e) 0.5 M KI.

Equations (10) and (11) were used to calculate the fill factor, *ff* and conversion efficiency, η of the cells.

$$ff = \frac{J_{max} \text{ x } V_{max}}{J_{sc} \text{ x } V_{oc}} \quad (10)$$

$$\eta = \frac{J_{sc} \text{ x } V_{oc} \text{ x } ff}{Incident\ power\ density} \quad (11)$$

where J_{max} and V_{max} are the current density and voltage at the point of maximum power output.

The performance parameters of DSSCs are summarized in Table 4. The highest J_{sc} of 5.56 mA cm^{-2} and η of 2.72% is observed for the cell containing the highest conducting electrolyte sample. This finding is in agreement with other researchers where performance of DSSCs is reported to be in correlation with the conductivity of polymeric electrolyte [27-31].

Table 4: Performance parameters of DSSCs.

KI content (M)	σ_{RT} (Scm^{-1})	V_{oc}(V)	J_{sc} (mA cm^{-2})	*ff*	η (%)
0.1	1.83 x 10^{-3}	0.66	3.73	0.47	1.16
0.2	2.72 x 10^{-3}	0.72	5.56	0.69	2.72
0.3	2.66 x 10^{-3}	0.67	4.89	0.67	2.03
0.4	2.64 x 10^{-3}	0.66	3.96	0.53	1.37
0.5	8.91 x 10^{-4}	0.65	2.72	0.50	0.88

4. Conclusion

Incorporation of KI has significantly increased the conductivity from 10^{-6} to 10^{-3} Scm^{-1}. The highest conductivity achieved was at 0.2 M of KI and highest photovoltaic performance achieved was 2.72%. The conductivity enhancement in PCL-DMF-KI electrolyte is due to the increase in the number, *n* and mobility, μ of ions. The temperature dependence of the exponent *s* was interpreted by the SPH model.

Acknowledgement

N.A.Y. Razamin would like to thank the Ministry of Higher Education Malaysia for MyBrainSc scholarship. The authors wish to thank Universiti Teknologi MARA for supporting this work through PERDANA 5/3 BESTARI (040/2018).

References

[1] A. Mahmood, "Recent research progress on quasi-solid-state electrolytes for dye-sensitized solar cells," *Journal of Energy Chemistry*, Vol. 24, No. 6, (2015), pp. 686-692.
[2] J. Wu *et al.*, "Progress on the electrolytes for dye-sensitized solar cells," *Pure and Applied Chemistry*, Vol. 80, No. 11, (2008), pp. 2241-2258.
[3] K. Rokesh, S. Anandan, and K. Jothivenkatachalam, "Polymer electrolytes in dye sensitized solar cells," *Materials Focus*, Vol. 4, No. 4, (2015), pp. 262-271.
[4] J. Wu *et al.*, "Electrolytes in dye-sensitized solar cells," *Chemical reviews*, Vol. 115, No. 5, (2015), pp. 2136-2173.
[5] A. M. C. Senevirathne, V. A. Seneviratne, O. A. Ileperuma, H. M. N. Bandara, and R. M. G. Rajapakse, "Novel Quasi-Solid-State Electrolyte Based on γ-Butyrolactone and Tetrapropylammonium Iodide for Dye-Sensitized Solar Cells Using Fumed Silica as the Gelling Agent," *Procedia Engineering*, Vol. 139, (2016), pp. 87-92.
[6] A. Nogueira, C. Longo, and M.-A. De Paoli, "Polymers in dye sensitized solar cells: overview and perspectives," *Coordination Chemistry Reviews*, Vol. 248, No. 13-14, (2004), pp. 1455-1468.
[7] Y. Shi *et al.*, "The electrically conductive function of high-molecular weight poly (ethylene oxide) in polymer gel electrolytes used for dye-sensitized solar cells," *Physical chemistry chemical physics*, Vol. 11, No. 21, (2009), pp. 4230-4235.
[8] M. G. Kang *et al.*, "Dye-sensitized TiO2 solar cells using polymer gel electrolytes based on PVdF-HFP," *Journal of The Electrochemical Society*, Vol. 151, No. 7, (2004), pp. E257-E260.
[9] H. Yang, M. Huang, J. Wu, Z. Lan, S. Hao, and J. Lin, "The polymer gel electrolyte based on poly (methyl methacrylate) and its application in quasi-solid-state dye-sensitized solar cells," *Materials chemistry and physics*, Vol. 110, No. 1, (2008), pp. 38-42.
[10] N. Yahya Wan Zaireen, T. Meng Wong, M. Khatani, E. Samsudin Adel, and M. Mohamed Norani, "Bio-based chitosan/PVdF-HFP polymer-blend for quasi-solid state electrolyte dye-sensitized solar cells," in *e-Polymers*, Vol. 17, (2017), pp. 355-362.
[11] F. Bella, J. R. Nair, and C. Gerbaldi, "Towards green, efficient and durable quasi-solid dye-sensitized solar cells integrated with a cellulose-based gel-polymer electrolyte optimized by a chemometric DoE approach," *RSC Advances*, Vol. 3, No. 36, (2013), pp. 15993-16001.
[12] X. Huang *et al.*, "A novel polymer gel electrolyte based on cyanoethylated cellulose for dye-sensitized solar cells," *Electrochimica Acta*, Vol. 80, (2012), pp. 219-226.
[13] D. Goldberg, "A review of the biodegradability and utility of poly (caprolactone)," *Journal of environmental polymer degradation*, Vol. 3, No. 2, (1995), pp. 61-67.
[14] H. J. Woo, C.-W. Liew, S. R. Majid, and A. K. Arof, "Poly(ε-caprolactone)-based polymer electrolyte for electrical double-layer

capacitors," *High Performance Polymers*, Vol. 26, No. 6, (2014), pp. 637-640.
[15] M. Ravi, S. Song, K. Gu, J. Tang, and Z. Zhang, "Electrical properties of biodegradable poly (ε-caprolactone): lithium thiocyanate complexed polymer electrolyte films," *Materials Science and Engineering: B*, Vol. 195, (2015), pp. 74-83.
[16] T. Winie, A. Azmar, and M. Rozana, "Ionic liquid effect for efficiency improvement in poly (methyl acrylate)/poly (vinyl acetate)-based dye-sensitized solar cells," *High Performance Polymers*, (2018), p. 0954008318770716.
[17] T. Winie and A. K. Arof, *Physical Chemistry of Macromolecules: Macro to Nanoscales*, Impedance spectroscopy: basic concepts and application for electrical evaluation of polymer electrolytes, 1st edn, Apple Academic Press, (2014), pp. 335–363.
[18] F. Muhammad, A. Jamal, and T. Winie, "Study on factors governing the conductivity performance of acylated chitosan-NaI electrolyte system," *Ionics*, Vol. 23, No. 11, (2017), pp. 3045-3056.
[19] A. K. Arof, S. Amirudin, S. Yusof, and I. Noor, "A method based on impedance spectroscopy to determine transport properties of polymer electrolytes," *Physical Chemistry Chemical Physics*, Vol. 16, No. 5, (2014), pp. 1856-1867.
[20] A. Jamal, F. Muhammad, A. Ali, and T. Winie, "Blends of hexanoyl chitosan/epoxidized natural rubber doped with EMImTFSI," *Ionics*, Vol. 23, No. 2, (2017), pp. 357-366.
[21] T. Winie and N. S. M. Shahril, "Conductivity enhancement by controlled percolation of inorganic salt in multiphase hexanoyl chitosan/polystyrene polymer blends," *Frontiers of Materials Science*, Vol. 9, No. 2, (2015), pp. 132-140.
[22] A. K. Jonscher, *Universal relaxation law: a sequel to Dielectric relaxation in solids*. Chelsea Dielectrics Press, (1996).
[23] M. Shukur, R. Ithnin, and M. Kadir, "Electrical characterization of corn starch-LiOAc electrolytes and application in electrochemical double layer capacitor," *Electrochimica Acta*, Vol. 136, (2014), pp. 204-216.
[24] M. Chai and M. Isa, "Investigation on the conduction mechanism of carboxyl methylcellulose-oleic acid natural solid polymer electrolyte," *International Journal of Advanced Technology & Engineering Research*, Vol. 2, No. 6, (2012), pp. 36-39.
[25] S. A. Mansour, I. Yahia, and F. Yakuphanoglu, "The electrical conductivity and dielectric properties of CI Basic Violet 10," *Dyes and Pigments*, Vol. 87, No. 2, (2010), pp. 144-148.
[26] T. Winie and A. K. Arof, "Dielectric behaviour and AC conductivity of $LiCF_3SO_3$ doped H-chitosan polymer films," *Ionics*, Vol. 10, No. 3-4, (2004), pp. 193-199.
[27] E. Aram, M. Ehsani, and H. Khonakdar, "Improvement of ionic conductivity and performance of quasi-solid-state dye sensitized solar cell using PEO/PMMA gel electrolyte," *Thermochimica Acta*, Vol. 615, (2015), pp. 61-67.
[28] H. Ng, S. Ramesh, and K. Ramesh, "Efficiency improvement by incorporating 1-methyl-3-propylimidazolium iodide ionic liquid in gel polymer electrolytes for dye-sensitized solar cells," *Electrochimica Acta*, Vol. 175, (2015), pp. 169-175.
[29] J. Theerthagiri, R. Senthil, M. Buraidah, J. Madhavan, and A. Arof, "Effect of tetrabutylammonium iodide content on PVDF-PMMA polymer blend electrolytes for dye-sensitized solar cells," *Ionics*, Vol. 21, No. 10, (2015), pp. 2889-2896.
[30] Y. Yang *et al*., "Effect of lithium iodide addition on poly (ethylene oxide)−poly (vinylidene fluoride) polymer-blend electrolyte for dye-sensitized nanocrystalline solar cell," *The Journal of Physical Chemistry B*, Vol. 112, No. 21, (2008), pp. 6594-6602.
[31] C. Bandarabnayake, G. Samarakkody, K. Perera, and K. Vidanapathirana, "Variation of performance of dye-sensitized solar cells with the salt concentration of the electrolyte," *Journal of Electrochemical Energy Conversion and Storage*, Vol. 13, No. 1, (2016) p. 011007.